Cancer Letters 469 (2020) 22–34

Contents lists available at ScienceDirect

Cancer Letters

journal homepage: www.elsevier.com/locate/canlet

Original Articles

Deubiquitinase PSMD14 enhances hepatocellular carcinoma growth and metastasis by stabilizing GRB2

Jie Lv[a,1], Sheng Zhang[b,1], Huita Wu[c,1], Jing Lu[a,1], Yuyan Lu[a], Fuqiang Wang[a], Wenxiu Zhao[a], Ping Zhan[a], Junjiang Lu[a], Qinliang Fang[a], Chengrong Xie[a,*], Zhenyu Yin[a,**]

[a] Department of Hepatobiliary Surgery, Zhongshan Hospital, Xiamen University, Fujian Provincial Key Laboratory of Chronic Liver Disease and Hepatocellular Carcinoma, Xiamen, Fujian, PR China
[b] Department of Pathology, Hubei Cancer Hospital, Tongji Medical College, Huazhong University of Science and Technology, Wuhan, Hubei, China
[c] Department of Oncology, Zhongshan Hospital, Xiamen University, Xiamen, Fujian, PR China

ARTICLE INFO

Keywords:
Deubiquitination
Protein stability
Posttranslational modification
OPA

ABSTRACT

Hepatocellular carcinoma (HCC) has emerged as one of the most common malignancies worldwide. It is associated with a high mortality rate, as evident from its increasing incidence and extremely poor prognosis. The deubiquitinating enzyme 26S proteasome non-ATPase regulatory subunit 14 (PSMD14) has been reported to act as an oncogene in several human cancers. The present study aimed to reveal the functional significance of PSMD14 in HCC progression and the underlying mechanisms. We found that PSMD14 was significantly upregulated in HCC tissues. Overexpression of PSMD14 correlated with vascular invasion, tumor number, tumor recurrence, and poor tumor-free and overall survival of patients with HCC. Knockdown and overexpression experiments demonstrated that PSMD14 promoted proliferation, migration, and invasion in HCC cells *in vitro*, and facilitated tumor growth and metastasis *in vivo*. Mechanistically, we identified PSMD14 as a novel posttranslational regulator of GRB2. PSMD14 inhibits degradation of GRB2 via deubiquitinating this oncoprotein in HCC cells. Furthermore, pharmacological inhibition of PSMD14 with O-phenanthroline (OPA) suppressed the malignant behavior of HCC cells *in vitro* and *in vivo*. In conclusion, our findings suggest that PSMD14 could serve as a novel promising therapeutic candidate for HCC.

1. Introduction

Hepatocellular carcinoma (HCC) is the fifth most common malignancy. It is the third leading cause of cancer-related deaths worldwide, with approximately 600,000 deaths per year [19]. Although systemic therapy for HCC, such as surgical resection, transarterial chemoembolization (TACE), local ablation, intra-arterial infusion chemotherapy, and molecular targeted therapy, has markedly advanced, the 5-year-survival rate remains less than 12%, owing to distant metastasis and recurrence [12,29]. Moreover, a large number of risk factors are associated with the initiation and progression of HCC. Therefore, it is essential to gain insight into the underlying mechanisms of HCC initiation and progression to design novel and effective therapies, with an aim to improve the prognosis of patients with HCC.

The deubiquitinase (DUB) 26S proteasome non-ATPase regulatory subunit 14 (PSMD14, also known as RPN11 and POH1), belongs to the JAMM domain metalloprotease family of DUBs and is a component of 19S regulatory cap in 26S proteasome. PSMD14 has been demonstrated to play important roles in regulating several biological processes, including protein stability [21], transcriptional regulation [23], aggresome clearance and disassembly [14], double-strand DNA break repair [8], senescence [9], embryonic stem cell differentiation [6], cellular viability [11], drug resistance [18,25] and metastasis [34]. Recently, overexpression of PSMD14 was reported in several kinds of human cancers, such as HCC, multiple myeloma, esophageal squamous cell carcinoma, and breast cancer, where it was associated with poor clinical outcomes in patients [17,25,30,33,34]. PSMD14 acts as an oncogene that promotes tumor progression by deubiquitinating different

* Corresponding author. Department of Hepatobiliary Surgery, Zhongshan Hospital of Xiamen University, Fujian Provincial Key Laboratory of Chronic Liver Disease and Hepatocellular Carcinoma, 209 South Hubin Road, Xiamen, 361004, Fujian Province, China.
** Corresponding author. Department of Hepatobiliary Surgery, Zhongshan Hospital of Xiamen University, Fujian Provincial Key Laboratory of Chronic Liver Disease and Hepatocellular Carcinoma, 209 South Hubin Road, Xiamen, 361004, Fujian Province, China.
E-mail addresses: eason_xiecr@126.com (C. Xie), yinzy@xmu.edu.cn (Z. Yin).
[1] These authors contributed equally to this work.

https://doi.org/10.1016/j.canlet.2019.10.025
Received 25 June 2019; Received in revised form 23 September 2019; Accepted 15 October 2019
0304-3835/ © 2019 Elsevier B.V. All rights reserved.

protein substrates. For instance, in esophageal squamous cell carcinoma, PSMD14 targets epithelial-mesenchymal transition (EMT)-associated transcription factor SNAIL for deubiquitination, thus stabilizing it and promoting tumor cell migration and invasion *in vitro* and tumor metastasis *in vivo* [34]. Similarly, in HCC, PSMD14 deubiquitylates transcriptional factor E2F1, increases its stability, and strengthens its downstream pro-survival signals, including upregulation of survivin and FOXM1 expression, thereby facilitating HCC growth [30]. Additionally, PSMD14 enhances metastatic capacity of HCC cells by deubiquitinating TGF-β receptors and caveolin 1 (CAV1), as well as negatively regulating the turnover of TGF-β receptors [31]. However, other mechanism of the contribution of PSMD14-mediated deubiquitination in the progression of HCC remains elusive.

In the present study, we examined the expression levels of PSMD14 in HCC tissues and analyzed the relationship of PSMD14 expression with clinicopathological features and prognosis of patients with HCC. Furthermore, we observed that PSMD14 promoted proliferation, migration, and invasion *in vitro* and tumor growth metastasis *in vivo* by stabilizing GRB2 protein. To summarize, our study reveals a previously unknown mechanism of the role of PSMD14 in HCC progression, wherein GRB2 expression is posttranslationally upregulated by PSMD14, resulting in tumor growth and metastasis.

2. Materials and methods

2.1. Tissue collection

Fifty-four pairs of HCC and corresponding adjacent normal liver tissues were obtained from patients with HCC who underwent hepatectomy between 2013 and 2017 at Zhongshan Hospital of Xiamen University. None of the patients received interventional therapy, chemotherapy, or sorafenib treatment before the surgery. Tissue samples were obtained and immediately frozen in liquid nitrogen and stored at −80 °C for further detection. Written informed consent for this research was obtained from all patients. The informed consent and experimental procedures were approved by the ethics committee of the Zhongshan Hospital of Xiamen University in accordance with the World Medical Association Declaration of Helsinki.

2.2. Cell culture

HEK293T, PLC/PRF/5, and Hep3B cells were acquired from the American Type Culture Collection (ATCC; Manassas, VA, USA). SMMC-7721 and MHCC-97h cells were obtained from the United Innovation of Mengchao Hepatobiliary Technology Key Laboratory of Fujian Province and Zhongshan Hospital of Fudan University, respectively. The authentication of these cell lines was performed via comparisons with the STR database. The cells were cultured in high glucose Dulbecco's modified Eagle medium (DMEM) supplemented with 10% fetal bovine serum (FBS; Serana, Germany) at 37 °C in a humidified incubator with 5% CO_2 in the air.

2.3. Immunohistochemistry

Tissues were fixed with 10% neutral formalin, embedded in paraffin, and 4-μm thick sections were prepared. In brief, immunohistochemistry (IHC) staining was performed as follows. The sections were deparaffinized, hydrated, and soaked in 3% H_2O_2 for 20 min at room temperature, and subsequently incubated with anti-PSMD14 (1:1000, ab10800, Abcam) and anti-GRB2 (1:1000, 10800-1-AP, Proteintech) antibodies at 4 °C overnight. The slides were incubated with biotinylated goat anti-rabbit antibodies for 1 h and stained with diaminobenzidine (DAB; Maixin Biotechnology, Fuzhou, China), followed by counterstaining with hematoxylin (Maixin Biotechnology). In order to avoid bias, the IHC-stained sections were evaluated by two clinical pathologists who were blinded to the experimental data. In brief, we counted 100 cells randomly at 200 × microscopic fields and classified them into five groups according to the percentage of positive staining cells in HCC tissues as follows: 0 = negative; 1–3 = 1–25%; 4–6 = 26–50%; 7–9 = 51–75%; 10–12 = ≥76%. The score ranging from 0 to 6 was considered as a low-expression group, whereas the score ranging from 7 to 12 was considered as a high-expression group.

2.4. Overexpression of PSMD14

Adenovirus-expressing vector and PSMD14-Flag (containing three Flag tags) were purchased from Vigene Biosciences Corporation (Jinan; Shandong Province, China). The cells were infected with adenovirus-expressing vector or PSMD14-Flag. After 48 h, the cells were used to detect the following.

2.5. Generation of knockdown cell lines

HCC cells were stably infected with shRNAs against PSMD14 (shPSMD14-1: GACACAGCAGAACAAGTCT, shPSMD14-2: CACTCAGC AGAGCTTTGAA), and GRB2 (shGRB2-1: GGTACAAGGCAGAGCTTAA, shGRB2-2: GAGCCAAGGCAGAAGAAAT), or scramble control in the pLV-shRNA-puro lentiviral background. Lentiviral particles were produced in HEK293T cells following the manufacturer's instructions (Inovogen Tech. Co., Beijing, China). Lentiviral particles were collected 48 h after transfection. The cells were infected with viral supernatants using polybrene (8 μg/mL). The stable cells were selected after 48 h using 5 μg/mL puromycin (InvivoGen) for one week.

2.6. Colony formation assay

The HCC cells were seeded at a density of 2×10^3 cells per well into 6-well culture plates in triplicate and then cultured for two weeks. Colonies formed were fixed with 4% paraformaldehyde for 20 min at room temperature. These were subsequently stained with 1% crystal violet for 30 min.

2.7. Cell proliferation detection

The HCC cells were seeded at a density of 2×10^3 cells per well into 96-well culture plates in triplicate. The proliferation of cells was assessed in three independent experiments using the CCK-8 (cell counting kit-8) assay (Dojindo; Beijing, China) at indicated time points according to the manufacturer's instructions. After 48 h, the cells were incubated with CCK-8 solution for 1.5 h. The absorbance of the colored solution was measured at 450 nm using a spectrophotometer.

2.8. Transwell assay

In order to detect cell migration and invasion, the indicated cells, mixed with 100 μL serum-free DMEM, were seeded onto an 8-μm pore polycarbonate membrane with or without pre-coated Matrigel in the upper chamber as per the manufacturer's instructions (Corning Incorporated; New York, NY, USA). The bottom chamber was filled with 600 μL DMEM, supplemented with 10% FBS. After 24 h incubation, the migratory or invasive cells were fixed with 4% paraformaldehyde for 20 min at room temperature, and subsequently stained with 1% crystal violet for 30 min. Cells in 10 randomly selected views were counted.

2.9. Mass spectrometry

The PLC/PRF/5 cells were incubated with 10 μM MG132 for 6 h. The cell lysates were immunoprecipitated with anti-PSMD14 antibodies (4197, Cell Signaling) overnight. Subsequently, these were conjugated with protein Dynabeads Protein G for immunoprecipitation (10001D, Invitrogen) for an additional incubation of 2 h. Gel electrophoresis was

run, following which in-gel digestion was performed to prepare samples for subsequent proteomic analysis. The LC-MS/MS analysis of the samples to identify proteins interacting with PSMD14 was conducted by College of Life Sciences, Xiamen University, as described below.

2.10. Protein extraction and western blotting

Cells were lysed in radioimmunoprecipitation assay (RIPA) lysis buffer (Beyotime; Beijing, China). After quantification using a BCA protein assay kit (Thermo), protein samples were separated by sodium dodecyl sulfate-polyacrylamide gel electrophoresis (SDS-PAGE). These were then transferred onto polyvinylidene difluoride (PVDF) membranes (Millipore). Membranes were blocked in 5% non-fat milk (Bio-Rad) for 1 h at room temperature and then incubated with anti-PSMD14 (4197, Cell Signaling), anti-β-actin (3700, Cell Signaling), or anti-GRB2 (ab32037, Abcam) antibody, followed by incubation with anti-rabbit or anti-mouse secondary antibodies conjugated to horseradish peroxidase (HRP, Jackson). Immunoreactive proteins were subsequently visualized using the enhanced chemiluminescence (ECL) detection system (Millipore).

2.11. Co-immunoprecipitation assay

HEK293T cells were seeded into 10-cm plates and transfected with indicated plasmids. Total proteins were extracted in co-immunoprecipitation (co-IP) lysis buffer (Beyotime, Beijing, China). The cell lysates were incubated with anti-GFP (ab32146, Abcam) or anti-HA (3724, Cell Signaling) antibody and Dynabeads Protein G for immunoprecipitation (10001D, Invitrogen) at 4 °C overnight. The beads were then washed thrice with lysis buffer and the immunoprecipitates were collected for Western blot analysis. For endogenous co-IP, lysates were incubated with 3 mg anti-PSMD14 (4197, Cell Signaling) or anti-GRB2 (ab32037, Abcam) antibody or negative control IgG (2729, Cell Signaling) overnight, followed by conjugation with protein Dynabeads Protein G for immunoprecipitation (10001D, Invitrogen) for an additional 2 h. After washing the beads thrice with lysis buffer, the immunoprecipitated proteins were collected for Western blot analysis.

2.12. In vivo deubiquitination assay

Indicated plasmids were transiently transfected into HEK293T cells for 48 h. After incubation with 10 μM MG132 (Selleck) for 6 h, the cells were harvested and lysed in the denature lysis buffer. HA-ubiquitinated FLAG-GRB2 was immunoprecipitated using the anti-FLAG M2 affinity gel (A2220, Sigma Aldrich). The FLAG-GRB2 protein was purified and immunoblotted with antibody against HA (5017, Cell Signaling).

Endogenous GRB2 was immunoprecipitated using the anti-GRB2 antibody (ab32037, Abcam) under denaturing conditions. The endogenous GRB2 protein was purified and subsequently collected for immunoblotting with antibody against ubiquitin (3936, Cell Signaling).

2.13. Animal study

A xenograft mouse model was constructed using 6-week-old male BALB/c athymic nude mice. A total of 2×10^7 cells were injected subcutaneously into the right flank of the nude mice. Approximately seven days later, tumor size was measured using a vernier caliper. Tumor volumes were calculated using formula $V = ½ (\text{length} \times \text{width}^2)$. To check the effect of PSMD14 on tumor metastasis, 2×10^6 cells were injected into the tail vein of male BALB/c athymic nude mice. Each group contained 7 mice and these mice were sacrificed eight weeks after injection. The lung tissues were fixed in 10% neutral formalin, embedded in paraffin, and cut into 3-μm thick sections. Hematoxylin and eosin (H&E) staining was performed in all lung tissues according to the standard protocol. The number of pulmonary metastasis nodules was counted under a microscope (Leica, Germany). All animal experiments were approved by the Animal Care and Use Committee of the Xiamen University.

2.14. Statistical analysis

All statistical analyses were performed using the SPSS software (Version 19.0). Data are presented as mean ± standard deviation (SD) and three independent experiments were performed. Differences in the results among groups were compared using Student's *t*-test or multi-way analysis of variance (ANOVA) test. The relationship between PSMD14 expression and clinical features of patients with HCC was analyzed using Chi-squared test. Spearman's rank correlation was used to examine the correlation between PSMD14 and GRB2 expression. The correlation between PSMD14 or GRB2 expression and prognosis of patients with HCC was analyzed using the Kaplan-Meier survival test and the log-rank test. Differences were considered significant for *p*-values less than 0.05.

3. Results

3.1. PSMD14 is highly expressed in HCC tissues

We first examined the expression levels of PSMD14 in 54 pairs of HCC and corresponding adjacent normal tissues using IHC assay. As shown in Figure 1A and 63.0% (34/54) HCC tissues expressed considerably higher PSMD14 levels than those expressed by adjacent normal liver tissues. To determine whether PSMD14 expression was related to the HCC progression, we analyzed the association between PSMD14 expression and clinicopathological features in these patients. Statistical analysis revealed a significant correlation between PSMD14 expression and vascular invasion ($p = 0.003$), tumor number ($p = 0.028$), and recurrence ($p < 0.001$) in the patients. However, PSMD14 expression was not associated with other factors, including age, gender, tumor size, differentiation, liver cirrhosis, serum HBV, and alpha-fetoprotein (AFP) level. Moreover, Kaplan-Meier and log-rank test analyses indicated that HCC patients with high PSMD14 expression had significantly decreased overall survival and tumor-free survival (Fig. 1B and C) than those with low PSMD14 expression. For further confirmation of these results, we analyzed The Cancer Genome Atlas (TCGA) data using the UALCAN online tool (http://ualcan.path.uab.edu/index.html). Consistent with our findings, these results showed that PSMD14 was significantly higher in primary HCC tissues than that in normal tissues (Fig. 1D). Additionally, the Kaplan-Meier analysis using the Kaplan-Meier Plotter online tool (http://kmplot.com/analysis/) demonstrated that patients with high PSMD14 expression exhibited significantly shorter overall survival compared with those having low PSMD14 expression ($p = 5.6e{-}05$, HR = 2.07 (1.44–2.98), Fig. 1E). Collectively, these data suggest that upregulation of PSMD14 was associated with malignant progression of HCC.

3.2. PSMD14 promotes HCC cell proliferation in vitro and tumor growth in vivo

To assess the functional role of PSMD14 in development and progression of HCC, we performed a knockdown of PSMD14 expression in SMMC-7721, PLC/PRF/5, and MHCC-97h cells using two shRNAs that targeted different sites within PSMD14 (Fig. 2A). The proliferation of HCC cells expressing PSMD14 shRNAs was significantly suppressed compared with that in the control cells (Fig. 2B). Similarly, colony formation analysis revealed that depletion of PSMD14 significantly inhibited the colony formation ability of HCC cells (Fig. 2C). Conversely, PSMD14 was overexpressed in PLC/PRF/5 and SMMC-7721 cells (Fig. 2D). CCK-8 and colony formation assays demonstrated a pro-proliferative effect of PSMD14 overexpression on HCC cells (Fig. 2E and F). The reciprocal effects of knockdown and overexpression of PSMD14 *in vitro* suggested that PSMD14 enhanced the proliferation

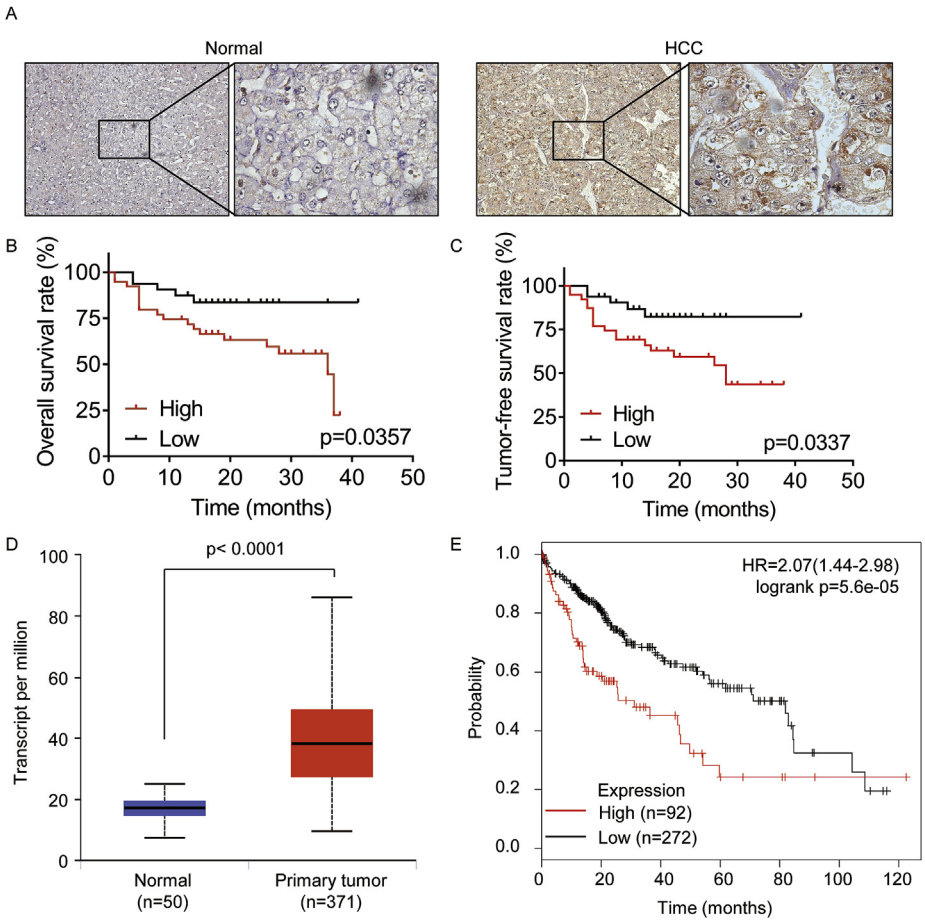

Fig. 1. Upregulation of PSMD14 predicts poor clinical outcome in patients with HCC.
A. The expression of PSMD14 in 54 pairs of HCC and corresponding adjacent normal liver tissues was examined by the immunohistochemistry (IHC) assay. A representative image is shown.
B and C. Kaplan-Meier survival analysis of the overall survival (B) and tumor-free survival (C) in the HCC patients based on PSMD14 expression. The low expression patients (n = 20) showed an expression value of HCC tissues less than the normal tissues, while the high expression patients (n = 34) showed the expression value of HCC tissues larger than normal tissues.
D. The PSMD14 mRNA levels in normal and primary HCC tumor tissues from the TCGA database. E. Kaplan-Meier survival analysis of the HCC patients from the TCGA database according to PSMD14 mRNA expression. The high expression patients showed the expression value of > 3rd quantile of PSMD14 expression, and the low expression patients showed the expression value < 3rd quartile of PSMD14 expression.

ability of HCC cells. The protein p53 has been demonstrated to be involved in PSMD14-mediated cell proliferation [33]. Nevertheless, we found that knockdown of PSMD14 led to an obvious decrease in the proliferation capacity of Hep3B cells (p53 deficient), indicating that PSMD14 promoted the proliferation of HCC cells via a p53-independent manner (Supplementary Fig. 1A and 1B).

To further confirm the proliferation potential of PSMD14 *in vivo*, the control and PSMD14-silenced MHCC-97h cells were subcutaneously injected into nude mice. The results showed that tumors formed by PSMD14 stable knockdown cells were much smaller than those formed by the control cells (Fig. 2G). Additionally, the tumor weight of the group was markedly lower than that of the control group (Fig. 2H). Collectively, these data demonstrated that PSMD14 promoted HCC growth both *in vitro* and *in vivo*.

3.3. PSMD14 promotes HCC cell migration and invasion in vitro and tumor metastasis in vivo

The correlation between PSMD14 expression and vascular invasion (Table 1) indicated that PSMD14 could be involved in HCC metastasis. We then validated the effects of PSMD14 on *in vitro* migratory and invasive behaviors of HCC cells. Transwell assay demonstrated that knockdown of PSMD14 dramatically decreased the migration and invasion capacity of SMMC-7721, PLC/PRF/5, and MHCC-97h cells as compared with that of control groups (Fig. 3A). Conversely, the cell migration and invasion ability was significantly enhanced by ectopic overexpression of PSMD14 in SMMC-7721 and PLC/PRF/5 cells (Fig. 3B).

To further validate the metastasis potential of PSMD14 *in vivo*, the control and PSMD14-silenced MHCC-97h cells were injected into the tail vein of nude mice to establish a metastasis model. It was observed that the knockdown of PSMD14 resulted in significantly decreased number and size of pulmonary metastatic nodules in mice (Fig. 3C). To conclude, these results demonstrated that PSMD14 facilitated cell migration and invasion, and tumor metastasis both *in vitro* and *in vivo*.

3.4. PSMD14 interacts with and deubiquitinates GRB2

To reveal the underlying mechanism of PSMD14 in regulating HCC progression, we performed a mass spectrometry analysis to identify global proteins that could co-immunoprecipitate with PSMD14. A total of 710 proteins were identified to potentially interact with PSMD14. Growth factor receptor-bound protein 2 (GRB2) is a key molecule in intracellular signal transduction and critical for cell cycle progression, motility, morphogenesis, and angiogenesis [13]. Moreover, GRB2 signaling has been implicated in tumorigenesis and cancer progression [20,24,27]. In this context, the interactome data of GRB2 from a previous study reported that PSMD14 is a potential interacting protein of GRB2 [4]. However, to date, whether GRB2 stability is regulated by DUBs has remained elusive. Interestingly, we found that GRB2 potentially interacted with PSMD14. A co-IP assay was utilized to validate the interaction between PSMD14 and GRB2 in HEK293T cells. The reciprocal co-IP experiment was subsequently performed to further define the interaction (Fig. 4A). Furthermore, the interaction between endogenous GRB2 and PSMD14 was confirmed by co-IP using PLC/PRF/5 cell lysate treated by proteasome inhibitor MG132 (Fig. 4B).

We then determined the regulatory relationship between PSMD14 and GRB2. The knockdown of PSMD14 significantly decreased the GRB2 protein expression in HCC cells (Fig. 4C). Moreover, xenografts in nude mice with MHCC-97h cells carrying PSMD14 knockdown displayed poor staining for GRB2 relative to that by control xenografts (Fig. 4D). However, depletion of PSMD14 could not have an effect on

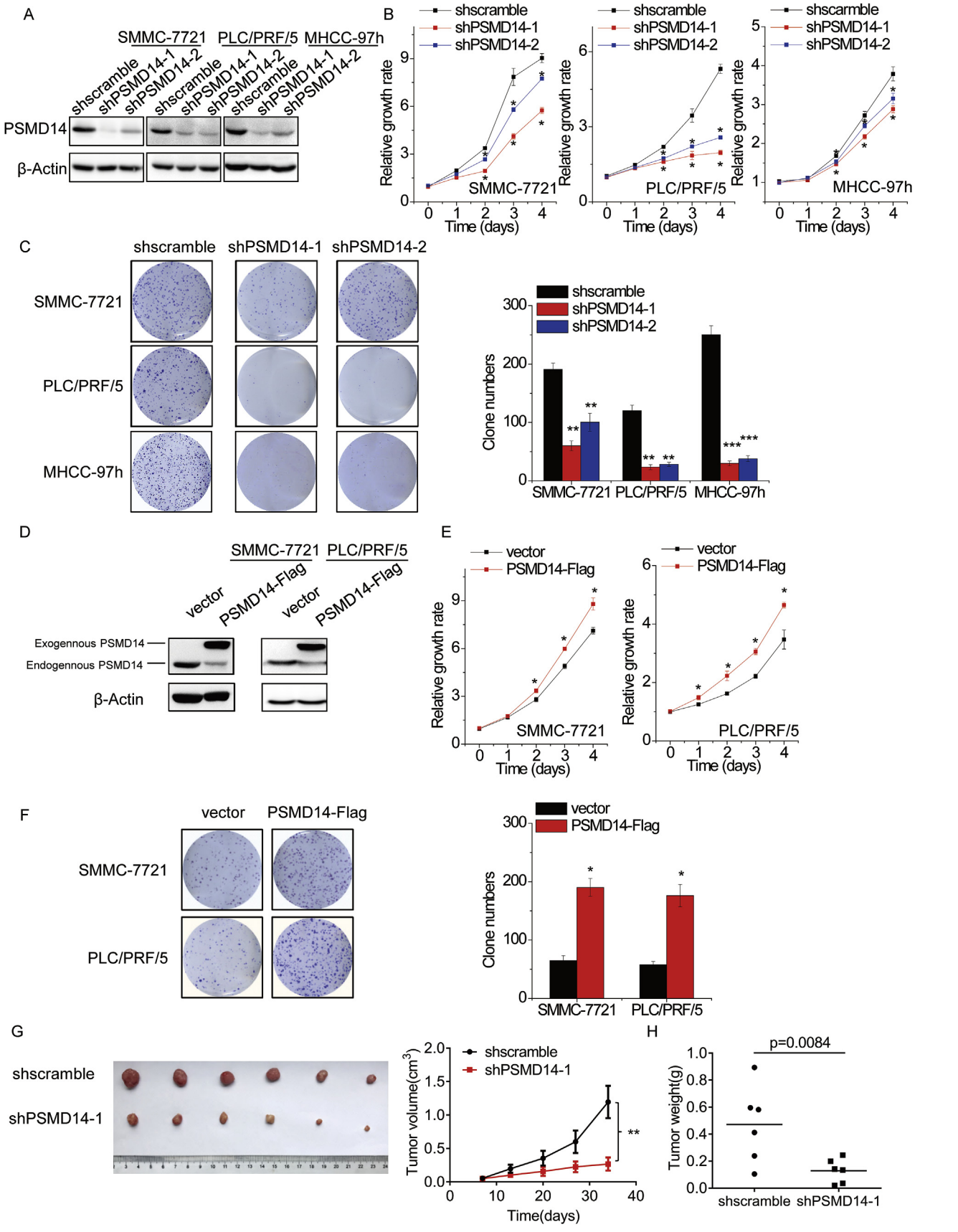

(caption on next page)

Fig. 2. PSMD14 promotes HCC growth *in vitro* and *in vivo*.
A. SMMC-7721, PLC/PRF/5 and MHCC-97h cells were infected with lentiviral particles expressing shRNAs targeting PSMD14. The knockdown efficacy was detected by the W
estern blot analysis.
B. The CCK-8 assay was used to detect the proliferation of control and PSMD14 knockdown HCC cells.
C. Colony formation assay was used to detect the proliferation of control and PSMD14 knockdown HCC cells.
D. SMMC-7721 and PLC/PRF/5 cells were infected with the adenovirus expressing vector or PSMD14-Flag (contains three Flag tags). The overexpression efficacy was detected by the Western blot analysis.
E. The CCK-8 assay was used to detect the proliferation of control and PSMD14 overexpressing SMMC-7721 and PLC/PRF/5 cells.
F. Colony formation assay was used to detect the proliferation of control and PSMD14 overexpressing SMMC-7721 and PLC/PRF/5 cells.
G. Scramble control or PSMD14 knockdown MHCC-97h cells were subcutaneously injected into nude mice for the observation of tumor growth.
H. The tumor weight of xenograft from the different groups (G) was calculated. *p < 0.05,**p < 0.01 and **p < 0.001. Data represent at least three independent sets of experiment.

Table 1
Association between PSMD14 expression and clinicopathological features of HCC.

Clinicopathological features	PSMD14 high	PSMD14 low	X^2	p value
Age(yr)[d]				
< 53	19(55.9%)	8(40.0%)	1.271	0.260
≥53	15(44.1%)	12(60.0%)		
Gender				
Male	28(82.4%)	16(80.0%)	0.046	0.830
Female	6(17.6%)	4(20.0%)		
Tumor size				
< 5 cm	9(26.5%)	8(40.0%)	1.069	0.301
≥5 cm	25(73.5%)	12(60.0%)		
Vascular invasion				
Yes	26(76.5%)	7(35.0%)	9.113	0.003*
No	8(23.5%)	13(65.0%)		
Differentiation				
Poor	5(14.7%)	0(0.0%)	3.317	0.190
Moderate	28(82.4%)	19(95.0%)		
Well	1 (2.9%)	1(5.0%)		
Liver cirrhosis status[a]				
No	13(44.8%)	13(72.2%)	3.372	0.066
Yes	16(55.2%)	5(27.8%)		
Serum HBV level (Iu/mL)[b]				
< 1000	23(69.7%)	11(55.0%)	1.170	0.279
≥1000	10(30.3%)	9(45.0%)		
Serum AFP level (ng/mL)				
< 200	17(50.0%)	13(65.0%)	1.148	0.284
≥200	17(50.0%)	7(35.0%)		
Tumor number				
Multiple	15(44.1%)	3(15.0%)	4.804	0.028*
Single	19(55.9%)	17(85.0%)		
Recurrence[c]				
Yes	19(79.2%)	4(23.5%)	12.508	< 0.001*
No	5(20.8%)	13(76.5%)		

*Statistically significant, P < 0.05.
[a] Seven missing data points.
[b] One missing data points.
[c] Thirteen missing data points.
[d] The mean age of the total 54 cases of patients was 53 years.

GRB2 mRNA expression levels (Supplementary Fig. 2A), indicating that PSMD14 modulated GRB2 expression through a post-transcriptional mechanism. To examine whether PSMD14 stabilized GRB2 protein, we checked the effect of both PSMD14 knockdown and overexpression on the stability of endogenous GRB2 protein by performing cycloheximide (CHX) pulse-chase assay. For this, HCC cells with PSMD14 alteration were treated with CHX to block protein synthesis at the indicated time, and subsequently, the GRB2 protein levels were analyzed using western blotting. It was observed that knockdown of PSMD14 accelerated the degradation of GRB2 protein in MHCC-97h cells (Fig. 4E), whereas PSMD14 overexpression could strikingly extend the half-life of GRB2 protein levels in PLC/PRF/5 cells (Fig. 4F). Since GRB2 is an important regulator of ERK, AKT, and STAT3 signaling pathways [2,7,26], we next investigated whether these signaling pathways were affected by PSMD14. We demonstrated that phosphorylation levels of AKT, ERK, and STAT3 were markedly decreased following PSMD14 knockdown (Supplementary Fig. 2B). Moreover, an *in vivo* ubiquitination assay validated that the ubiquitination level of GRB2 was significantly increased by PSMD14 silencing (Fig. 4G), thereby protecting GRB2 from degradation. We next determined which types of polyubiquitin modifications of GRB2 protein were affected by PSMD14-mediated deubiquitination. For this, HEK293T cells were transfected with FLAG-GRB2 and GFP-PSMD14, and each one of the different ubiquitins (K11-, K48-, or K63-only ubiquitin-HA), separately. Next, FLAG-GRB2 proteins in the lysates were purified and subjected to Western blot analysis using an anti-HA antibody. K48- and K63-linked ubiquitination on GRB2 was substantially reduced by the overexpression of PSMD14 (Fig. 4H). Previous reports demonstrated that the C120 and H113 sites and the JAMM motif of PSMD14 are critical for the deubiquitinating enzymatic activity of PSMD14 [30]. Moreover, we found that the mutant PSMD14 could interact with GRB2 (Supplementary Fig. 2C), and only ectopic expression of wild-type PSMD14, but not the PSMD14 mutants C120S or H113Q or △JAMM (deletion of JAMM motif), upregulated the GRB2 protein levels (Supplementary Fig. 2D), suggesting that the deubiquitinating enzymatic activity of PSMD14 was essential for regulating the expression of GRB2. Taken together, these data demonstrated that PSMD14 mediated GRB2 deubiquitination and stabilization.

3.5. PSMD14 exerts oncogenic effects through GRB2

We next examined whether PSDM14 regulated HCC progression in a GRB2-dependent manner. Endogenous GRB2 was silenced by transfection of lentiviral particles expressing GRB2 shRNAs in HCC cells. The knockdown efficacy was validated by immunoblot analysis (Fig. 5A). CCK-8 and colony formation assays demonstrated that depletion of GRB2 suppressed cell proliferation compared with that in the control groups. Moreover, knockdown of GRB2 inhibited HCC cell migration and invasion, as evident from results of the transwell assays (Fig. 5D). In addition, we rescued the expression of GRB2 in PSMD14-silenced HCC cells. The restoration of GRB2 expression abolished the inhibition of the proliferative, migratory, and invasive abilities induced by PSMD14 depletion (Fig. 5E and F, Supplementary Fig. 3A and 3B). Interestingly, rescuing the activation of AKT, ERK, or STAT3 signaling alone also partially attenuated the PSMD14 silencing-mediated suppressive effects (Supplementary Fig. 3C and 3D). Taken together, these findings suggested that PSMD14 functions upstream of GRB2 to regulate HCC progression.

3.6. PSMD14 expression is positively correlated with GRB2 in HCC tissues and predicts poor clinical outcome

Based on our experimental findings on HCC cell lines that PSMD14 could increase GRB2 expression, we performed IHC staining of GRB2 on the same set of HCC tissues to determine the relevance of regulation of GRB2 expression by PSMD14 in the patients. As shown in Fig. 6A, GRB2 expression was considerably higher in HCC tissues than that in the adjacent normal liver tissues. Furthermore, we found that the

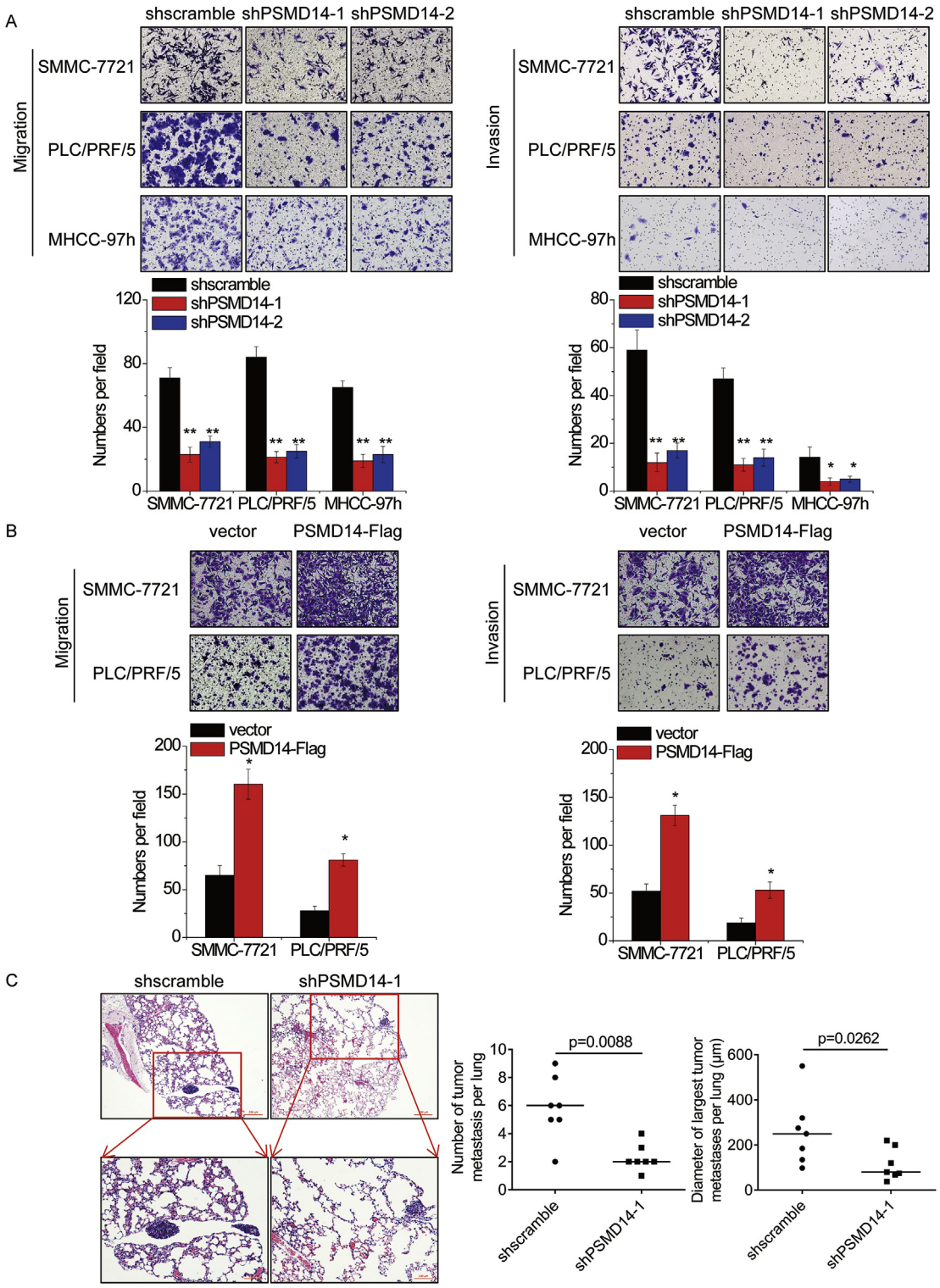

Fig. 3. PSMD14 facilitates HCC invasion and metastasis *in vitro* and *in vivo*.

A. The representative images of transwell assay for the control and PSMD14 knockdown HCC cells. The cells were counted under a microscope in five randomly selected fields.

B. The representative images of transwell assay for the control and PSMD14 overexpressing SMMC-7721 and PLC/PRF/5 cells. The cells were counted under a microscope in five randomly selected fields.

C. The representative microscopic images of pulmonary metastatic lesions at eight weeks after the injection of indicated MHCC-97h cells into the tail vein of nude mice. The number and diameter of lung metastatic tumors in each group were determined. *p < 0.05 and **p < 0.01. Data represent at least three independent sets of the experiment.

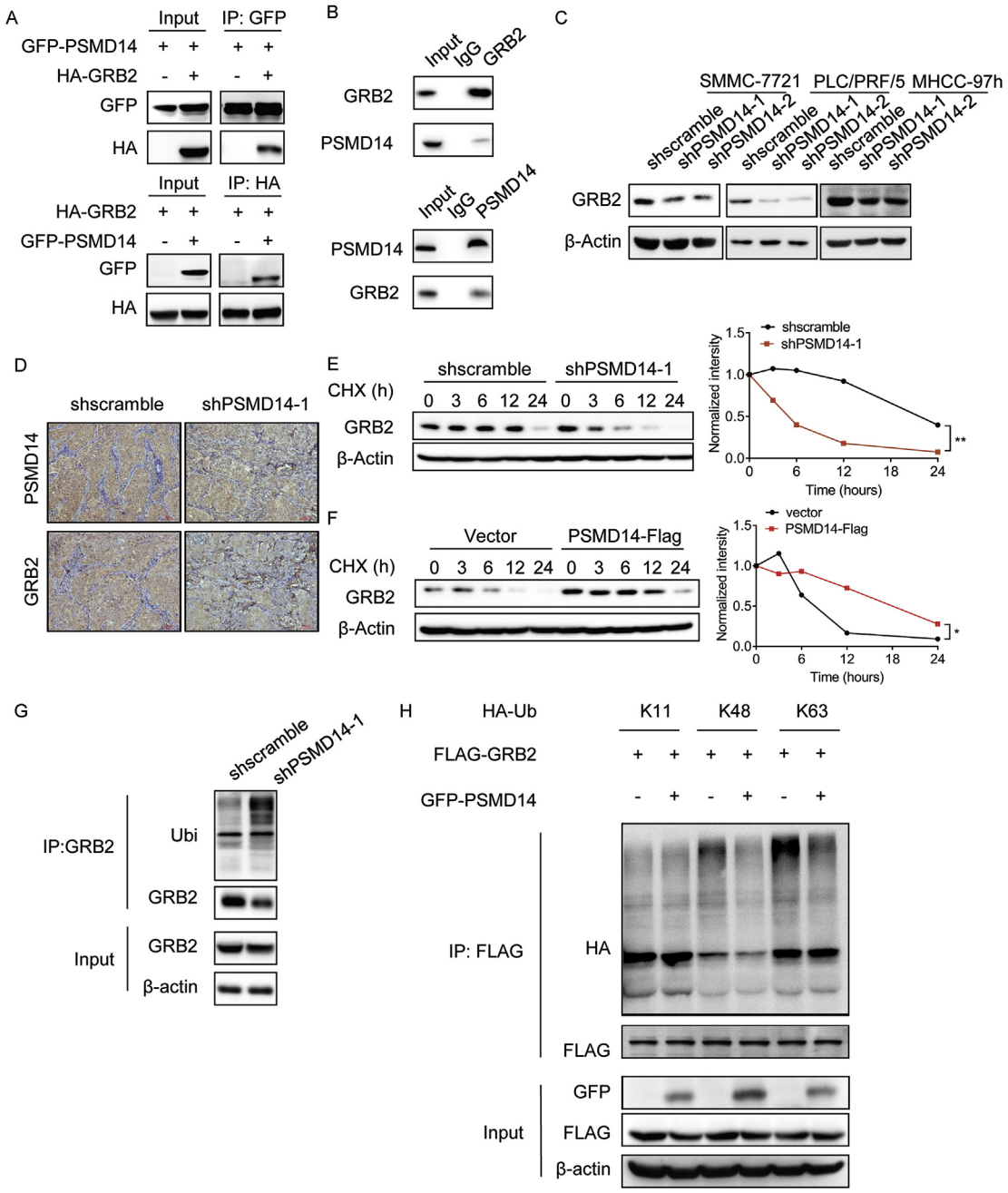

Fig. 4. PSMD14 deubiquitinates and stabilizes GRB2.

A. The GFP-PSMD14 plasmid was co-transfected with HA-GRB2 plasmid into HEK293T cells. The cell lysates were immunoprecipitated to pull down GRB2 or PSMD14 by the anti-HA or anti-GFP antibodies, respectively, and subjected to immunoblotting.

B. Endogenous GRB2 proteins were immunoprecipitated with anti-GRB2 antibody and then analyzed by immunoblotting (up panel). Endogenous PSMD14 proteins wereimmunoprecipitated with anti-PSMD14 antibody and then analyzed by immunoblotting (down panel). The IgG antibody was used as the control.

C. The expression levels of GRB2 in the control and PSMD14 knockdown HCC cells were determined by the Western blot.

D. Immunohistochemical staining for GRB2 and PSMD14 in tumor xenografts of nude mice developed by PSMD14 knockdown of the MHCC-97h cells.

E. The control and PSMD14 knockdown MHCC-97h cells were treated with CHX (100 μg/mL) for the indicated time points. The cell lysates were subjected to immunoblotting (left panel) and the GRB2 expression was quantified by Quantity One software (right panel). **$p < 0.01$.

F. Control and PSMD14 overexpressing PLC/PRF/5 cells were treated with CHX (100 μg/mL) for the indicated time points. The cell lysates were subjected to immunoblotting (left panel) and GRB2 expression was quantified by Quantity One software (right panel). *$p < 0.05$.

G. The control and PSMD14 knockdown MHCC-97h cells were treated with MG132 at 10 μM for 8 h. The cell lysates were then immunoprecipitated with anti-GRB2 antibody, and the immunocomplexes were immunoblotted with anti-GRB2 and anti-ubiquitin antibodies.

H. HEK293T cells overexpressing FLAG-GRB2, GFP-PSMD14, and HA-tagged different forms of ubiquitin were treated with MG132 (10 μM) for 8 h. The cell lysates were immunoprecipitated by using anti-FLAG M2 affinity gel. The ubiquitination levels of GRB2 were detected using anti-HA antibody.

overexpression of PSMD14 in HCC tissues was accompanied by upregulation of GRB2 as compared with that in the normal liver tissues (Fig. 6B, $p < 0.0001$, $R = 0.479$). Moreover, we observed a strong positive correlation between PSMD14 and GRB2 expression in the same HCC samples (Fig. 6C, $p < 0.0001$, $R^2 = 0.3987$).

To investigate the prognostic value of GRB2 expression, the

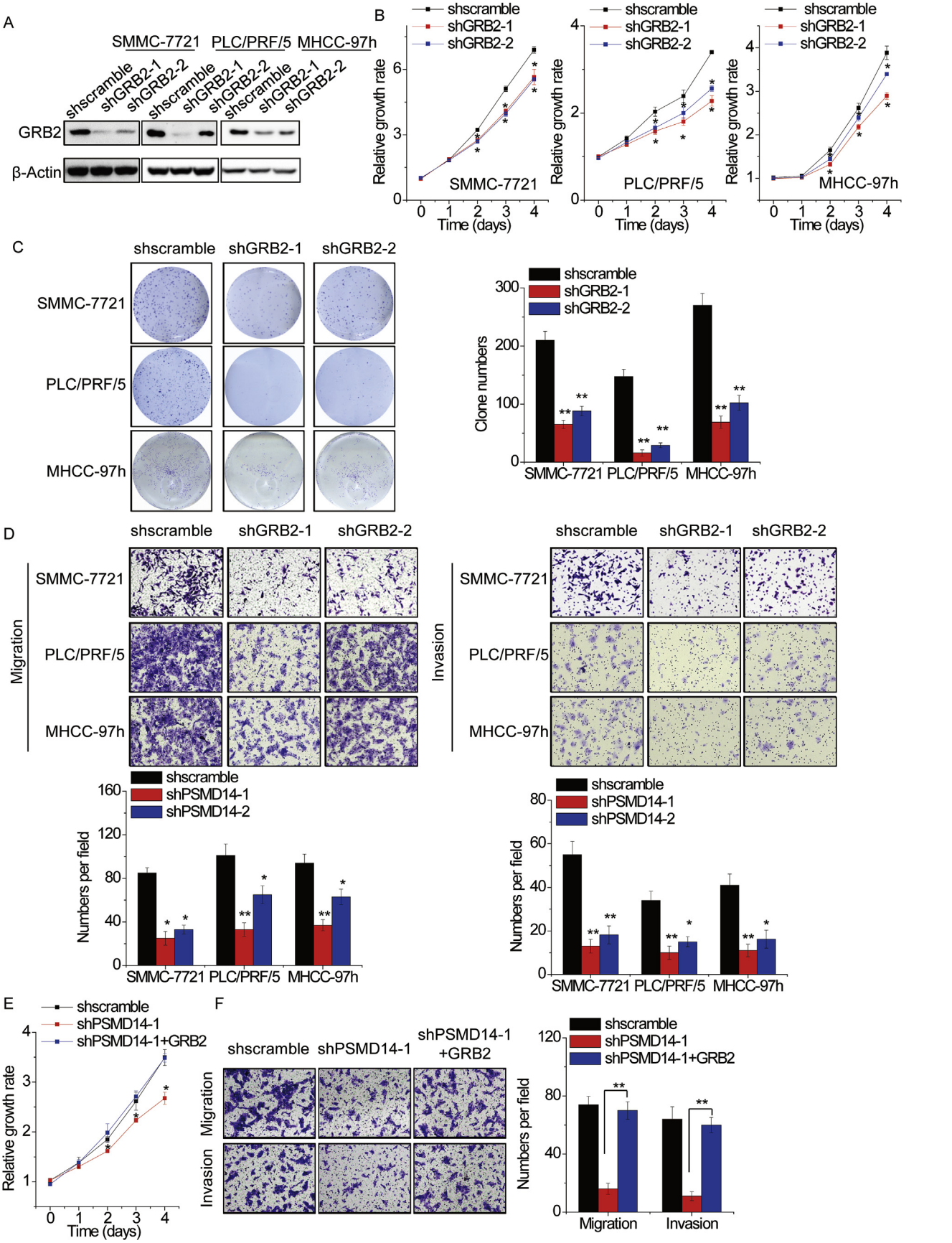

(caption on next page)

Fig. 5. PSMD14 exerts oncogenic effects through GRB2.
A. SMMC-7721, PLC/PRF/5, and MHCC-97h cells were infected with lentiviral particle expressing shRNAs targeting GRB2. The knockdown efficacy was detected by the Western blot analysis.
B. The CCK-8 assay was used to detect the proliferation of control and GRB2 knockdown HCC cells.
C. Colony formation assay was used to detect the proliferation of control and PSMD14 knockdown HCC cells.
D. The representative images of transwell assay on for the control and PSMD14 knockdown HCC cells. The cells were counted under a microscope in five randomly selected fields.
E. GRB2 abolished the proliferation inhibition induced by PSMD14 knockdown in MHCC-97h cells as confirmed by CCK-8 assays.
F. GRB2 abolished the migration and invasion inhibition induced by PSMD14 knockdown in MHCC-97h cells as confirmed by transwell assays. *p < 0.05 and **p < 0.01. Data represent at least three independent experiments.

association of GRB2 protein expression with clinical outcomes of HCC patients was analyzed. The Kaplan–Meier analysis revealed that patients with high GRB2 expression in HCC tissues had a shorter overall postoperative survival time than those with low expression ($p = 0.0281$, Fig. 6D). Additionally, the effects of the combination of GRB2 and PSMD14 expression on outcomes are shown in Fig. 6E. PSMD14 & GRB2 high group had a worse outcome than the PSMD14 & GRB2 low group ($p = 0.0241$). Taken together, our results suggested that the overexpressed PSMD14 and GRB2 could serve as potential prognostic markers for patients with HCC.

3.7. Therapeutic effects of PSMD14 inhibitor OPA on the malignant behavior of HCC cells

Recently, a metallopeptidase inhibitor O-phenanthroline (OPA) was found to inhibit PSMD14 activity, thereby suppressing cell growth and

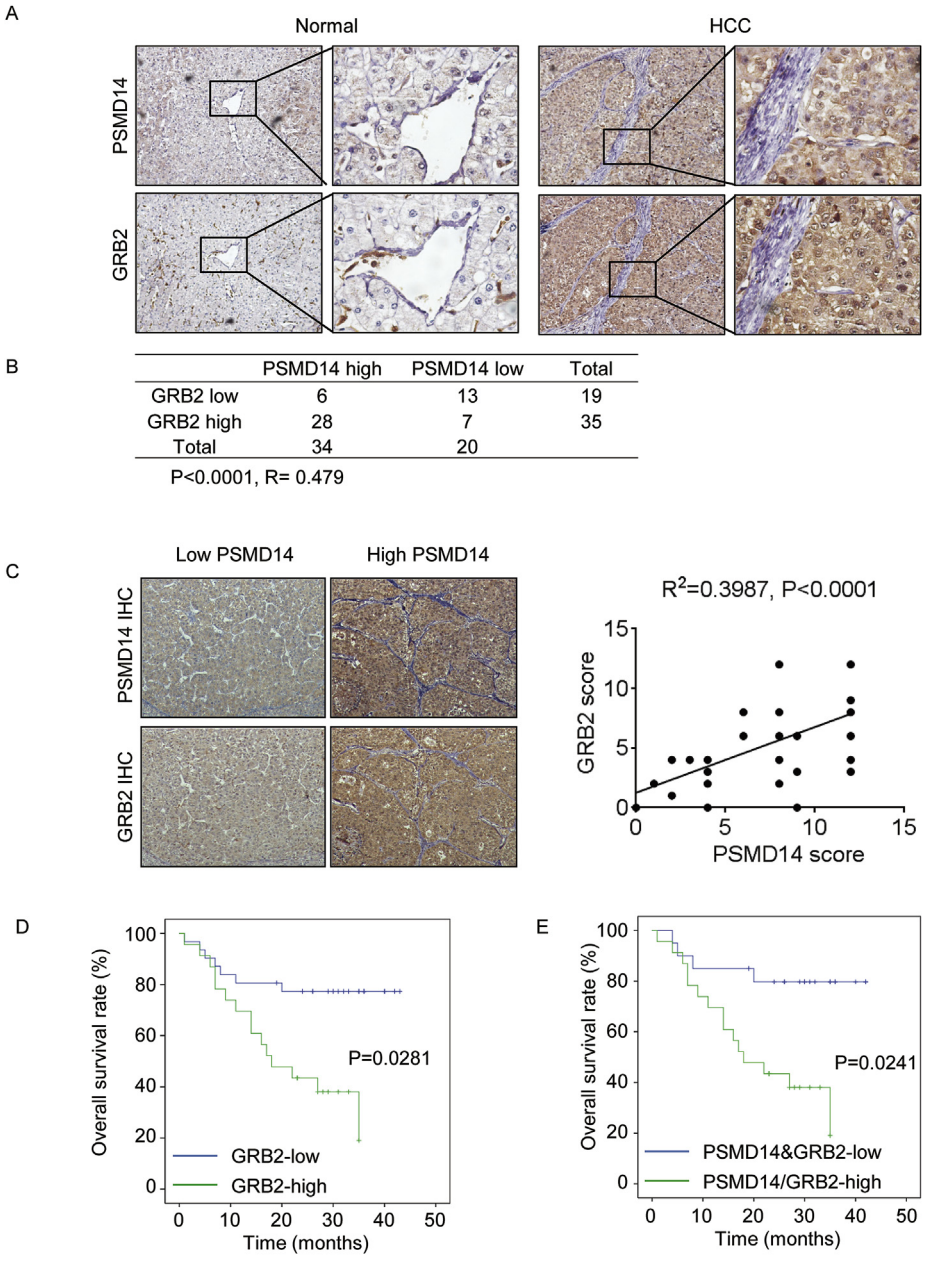

Fig. 6. PSMD14 expression is positively correlated with GRB2 in HCC tissues.
A. The representative images of immunohistochemical staining of PSMD14 and GRB2 in the same normal and HCC tissues.
B. Correlation study of PSMD14 and GRB2 in HCC tissues. Statistical analyses were performed with the Chi-square test. R, Pearson correlation coefficient.
C. Representative images of immunohistochemical staining of GRB2 in HCC tissues with different expression levels of PSMD14. Scatter diagram exhibited a positive correlation of PSMD14 and GRB2 in HCC tissues by IHC.
D. Survival analysis of HCC patients by Kaplan-Meier plots and log-rank tests. The patients were categorized into the high and low expression groups of GBR2 based on IHC staining.
E. Survival analysis of HCC patients by Kaplan-Meier plots and log-rank tests. The patients were categorized into the high and low expression groups of GBR2 and PSMD14 based on IHC staining.

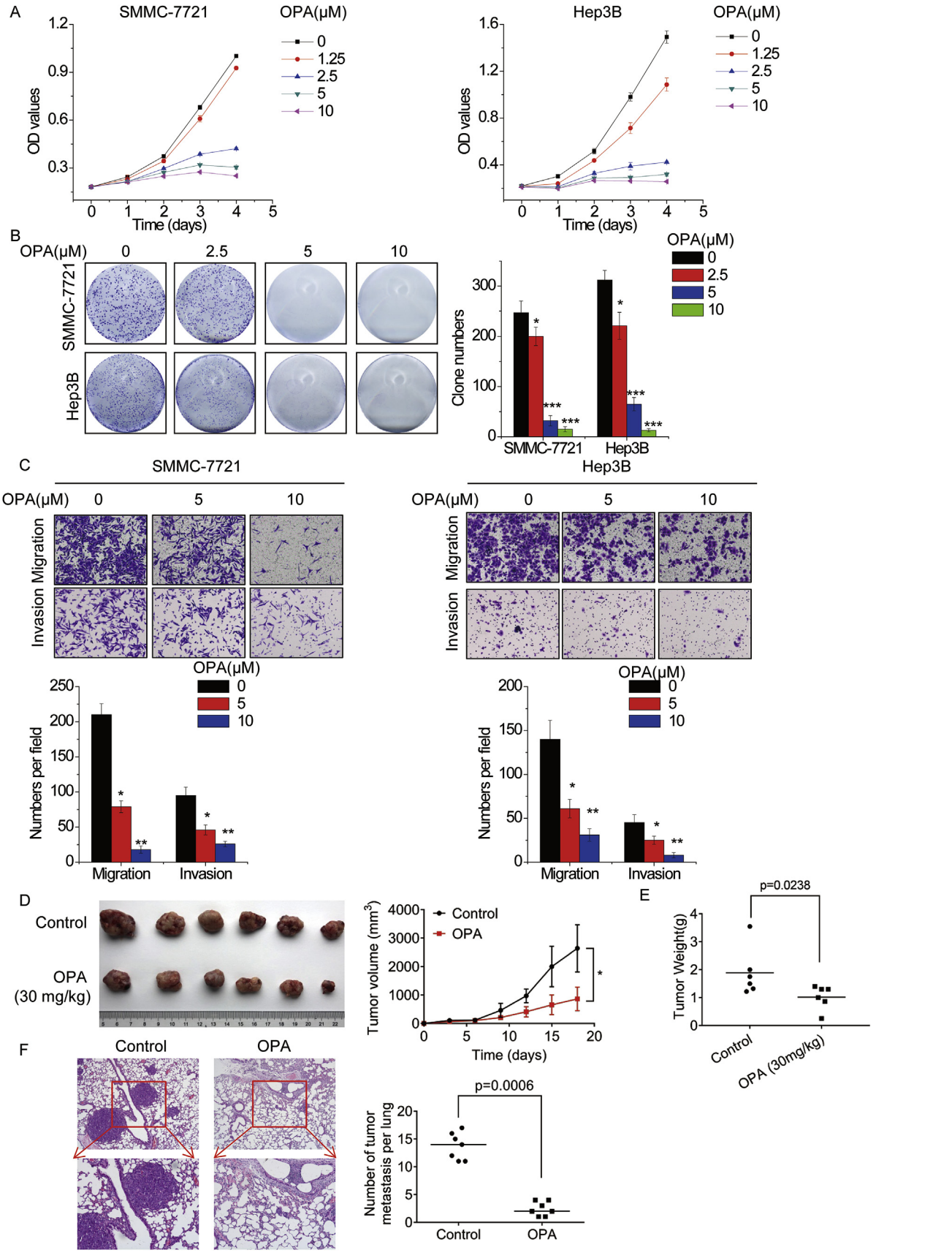

(caption on next page)

Fig. 7. Therapeutic effects of PSMD14 inhibitor OPA on the malignant behavior of HCC cells.
A. The cytotoxicity of various concentrations of OPA to SMMC-7721 and Hep3B cells was examined by CCK-8 assay.
B. The cytotoxicity of various concentrations of OPA to SMMC-7721 and Hep3B cells was examined by colony formation assay.
C. SMMC-7721 and Hep3B cells were pre-treated with different concentrations of OPA for 48 h. A transwell assay was then conducted to examine the cell migration and invasion. The representative images (up panel) and statistical results of the transwell assay.
D. Nude mice with tumors formed by SMMC-7721 cells were treated with vehicle control or OPA (30 mg/kg; intraperitoneal (i.p.), 3 times each week) for 20 days.
E. The tumor weight of xenograft from different groups (D) was calculated.
F. SMMC-7721 cells were injected into the tail vein of nude mice. These nude mice were then treated with vehicle control or OPA (30 mg/kg; intraperitoneal (i.p.), 3 times each week). After 6 weeks, the representative microscopic images of pulmonary metastatic lesions were shown. The number of lung metastatic tumors in each group was calculated. *p $<$ 0.05, **p $<$ 0.01, and ***p $<$ 0.001. Data represent at least three independent experiments.

overcoming drug resistance [25]. We next evaluated the therapeutic effect of OPA on HCC. SMMC-7721 and Hep3B cells were treated with different concentrations of OPA. The results of CCK-8 and colony formation assays showed that the treatment of OPA inhibited the proliferation of HCC cells in a concentration-dependent manner (Fig. 7A and B). Furthermore, the migration and invasion of SMMC-7721 and Hep3B cells was markedly reduced upon treatment with different concentrations of OPA when compared to the DMSO-treated cells (Fig. 7C). Moreover, we examined whether OPA affected the HCC growth and metastasis *in vivo*. It was demonstrated that treatment of OPA resulted in an obvious decrease in tumor growth and metastasis in nude mice (Fig. 7D–G). Taken together, these data indicated a strong inhibitory effect of PSMD14 inhibitor OPA on HCC progression.

4. Discussion

In the present study, our results demonstrated that PSMD14 was overexpressed in HCC tissues, and was significantly associated with vascular invasion, tumor number, and tumor recurrence. Furthermore, it was found that the upregulation of PSMD14 expression predicted shorter overall and tumor-free survival time in patients with HCC. Consistent with these results, the high PSMD14 expression in patients with HCC of the TCGA database suggested a trend of poor prognosis. Previous studies revealed a significant negative correlation between PSMD14 expression and survival time of patients with different cancers, including HCC, breast cancer, esophageal cancer, multiple myeloma, and colorectal cancer [17,25,33,34]. Our results are in accordance with these studies, implying that PSMD14 could be a potential prognostic predictor for patients with these cancers.

As a deubiquitinase, overexpression of PSMD14 has been found to contribute to cancer progression through deubiquitinating and stabilizing diverse substrates. Here, our findings showed that PSMD14 promoted *in vitro* proliferation, migration, and invasion of HCC cells, and facilitated tumor growth and metastasis *in vivo*. Considering that GRB2 played a critical role in enhancing the malignant behavior of cancer cells [13], and the ubiquitination of GRB2 remains elusive, we revealed the mechanism underlying PSMD14-mediated GRB2 regulation. We found that PSMD14 increased the protein levels of GRB2; however, it did not influence the mRNA levels of GRB2. Moreover, the downstream signaling of GRB2 was affected by PSMD14 knockdown. The knockdown of PSMD14 accelerated the degradation of GRB2 protein, whereas PSMD14 overexpression could strikingly extend the half-life of GRB2 protein levels. Additionally, the ubiquitination level of GRB2 was significantly increased by depletion of PSMD14. PSMD14 belongs to the JAMM domain metalloproteases and functions as a K63-specific deubiquitinase [17]. However, both K48- and K63-linked ubiquitination on GRB2 were substantially reduced by overexpression of PSMD14. The decreased K48-linked ubiquitination on GRB2 by PSMD14 was considerably obvious than the K63-linked ubiquitination, indicating that an indirect mechanism was involved in the regulation of PSMD14-mediated K48-linked ubiquitination of GRB2. A recent study reported a similar phenomenon that both K48 and K63 poly-ubiquitin chains of TGFBR1 and TGFBR2 proteins could be reduced by PSMD14. PSMD14 modulated K48 poly-ubiquitin chains of TGFBR1 and TGFBR2 in a lysosomal degradation-dependent manner through deubiquitinating CAV1 [32]. Based on this research, we speculated that PSMD14 could affect some intermediate proteins that could regulate K48-linked ubiquitination on GRB2. The exact molecular mechanism by which PSMD14 regulates the K48-linked ubiquitination on GRB2 warrants further investigation.

Tumor metastasis is the primary cause of poor clinical outcomes in patients with HCC [3]. Snail1 is a zinc-finger transcription factor and crucial for cellular movement during cancer metastasis by inducing epithelial-mesenchymal transition (EMT) [5]. The upregulation of Snail1 expression is related to poor prognosis of patients with cancer [15]. Snail1 directly represses epithelial markers, such as E-cadherin and claudins, by forming a transcriptional complex with epigenetic modifiers, such as DNA methylation transferases (DNMTs), EZH2, and G9a [10,28]. It has been reported that PSMD14 is critical for Snail1-induced migration, invasion, and the EMT process in esophageal cancer cells. PSMD14 was identified to associate with Snail1, which could induce deubiquitination and stabilization of Snail1 protein [34]. The cytokine transforming growth factor β (TGF-β) signaling induces EMT and enhances the metastatic potential of cancer cells through induction of Snail1 expression [1]. Interestingly, PSMD14 could deubiquitinate TGF-β receptors and CAV1, and subsequently suppress lysosome pathway-mediated turnover of TGF-β receptors in HCC cells, which is critical for TGF-β signaling [32]. GRB2 is an adaptor protein that interacts with phosphorylated TGF-β receptor. A recent study demonstrated that Snail1 expression was upregulated by GRB2 overexpression and was further enhanced by TGF-β stimulation in lung cancer cells [20]. Our results showed that PSMD14 could stabilize GRB2 and upregulate its expression, suggesting that PSMD14 might also increase Snail1 expression through GRB2. Based on these findings, we suspected that EMT-related transcription factor Snail1 could be crucial for PSMD14-induced metastasis via GRB2 and TGF-β signaling.

Recently, specific, small-molecule inhibitors against PSMD14, including OPA, 8-thioquinoline (8TQ), and capzimin, have been identified. Some inhibitors have been shown to suppress cancer progression. OPA blocks cellular proteasome function, induces apoptosis in multiple myeloma cells, and overcomes resistance to proteasome inhibitor bortezomib [25]. 8TQ can suppress the proliferation of tumor cells in culture [22]. As a derivative of 8TQ, capzimin exhibits higher selectivity for PSMD14 over the related JAMM proteases and several other metalloenzymes. According to a study, capzimin induced an unfolded protein response and inhibited the proliferation and resistance of cancer cells to bortezomib [16]. Herein, we evaluated the therapeutic effects of OPA in malignant phenotypes of HCC cells and found that it could significantly inhibit HCC growth and metastasis *in vitro* and *in vivo*, indicating that targeting PSMD14 could serve as a potential therapeutic modality for HCC.

In summary, the present study demonstrated that overexpression of PSMD14 indicates the poor prognosis of patients with HCC, and PSMD14-mediated GRB2 stabilization enhanced HCC growth and metastasis. These findings provided the rationale for considering PSMD14 as a novel prognostic predictor and therapeutic target for HCC.

Declaration of competing interest

None.

Acknowledgement

This work was supported by the National Natural Science Foundation of China (No.81672418, 81702351, 81871961, 81702348, 81871963, 81871910 and 81572335), the Natural Science Foundation of Fujian (No.2017-2-101, 2018J01389, 2018J01398, 2016-2-80), Research Project of health and family planning (no. 2018-2-64 and 2018-ZQN-84).

Appendix A. Supplementary data

Supplementary data to this article can be found online at https://doi.org/10.1016/j.canlet.2019.10.025.

References

[1] R.J. Akhurst, A. Hata, Targeting the TGFbeta signalling pathway in disease, Nat. Rev. Drug Discov. 11 (2012) 790–811.
[2] T. Araki, H. Nawa, B.G. Neel, Tyrosyl phosphorylation of Shp2 is required for normal ERK activation in response to some, but not all, growth factors, J. Biol. Chem. 278 (2003) 41677–41684.
[3] R. Bhatia, S. Ravulapati, A. Befeler, J. Dombrowski, S. Gadani, N. Poddar, Hepatocellular carcinoma with bone metastases: incidence, prognostic significance, and management-single-center experience, J. Gastrointest. Cancer 48 (2017) 321–325.
[4] M. Brehme, O. Hantschel, J. Colinge, I. Kaupe, M. Planyavsky, T. Kocher, K. Mechtler, K.L. Bennett, G. Superti-Furga, Charting the molecular network of the drug target Bcr-Abl, Proc. Natl. Acad. Sci. U.S.A. 106 (2009) 7414–7419.
[5] M. Brzozowa, M. Michalski, G. Wyrobiec, A. Piecuch, A. Dittfeld, M. Harabin-Slowinska, D. Boron, R. Wojnicz, The role of Snail1 transcription factor in colorectal cancer progression and metastasis, Contemp. Oncol. 19 (2015) 265–270.
[6] S.M. Buckley, B. Aranda-Orgilles, A. Strikoudis, E. Apostolou, E. Loizou, K. Moran-Crusio, C.L. Farnsworth, A.A. Koller, R. Dasgupta, J.C. Silva, M. Stadtfeld, K. Hochedlinger, E.I. Chen, I. Aifantis, Regulation of pluripotency and cellular reprogramming by the ubiquitin-proteasome system, Cell stem cell 11 (2012) 783–798.
[7] T. Burdon, A. Smith, P. Savatier, Signalling, cell cycle and pluripotency in embryonic stem cells, Trends Cell Biol. 12 (2002) 432–438.
[8] L.R. Butler, R.M. Densham, J. Jia, A.J. Garvin, H.R. Stone, V. Shah, D. Weekes, F. Festy, J. Beesley, J.R. Morris, The proteasomal de-ubiquitinating enzyme POH1 promotes the double-strand DNA break response, EMBO J. 31 (2012) 3918–3934.
[9] A. Byrne, R.P. McLaren, P. Mason, L. Chai, M.R. Dufault, Y. Huang, B. Liang, J.D. Gans, M. Zhang, K. Carter, T.B. Gladysheva, B.A. Teicher, H.P. Biemann, M. Booker, M.A. Goldberg, K.W. Klinger, J. Lillie, S.L. Madden, Y. Jiang, Knockdown of human deubiquitinase PSMD14 induces cell cycle arrest and senescence, Exp. Cell Res. 316 (2010) 258–271.
[10] C. Dong, Y. Wu, J. Yao, Y. Wang, Y. Yu, P.G. Rychahou, B.M. Evers, B.P. Zhou, G9a interacts with Snail and is critical for Snail-mediated E-cadherin repression in human breast cancer, J. Clin. Investig. 122 (2012) 1469–1486.
[11] M. Gallery, J.L. Blank, Y. Lin, J.A. Gutierrez, J.C. Pulido, D. Rappoli, S. Badola, M. Rolfe, K.J. Macbeth, The JAMM motif of human deubiquitinase Poh1 is essential for cell viability, Mol. Cancer Ther. 6 (2007) 262–268.
[12] Y.A. Ghouri, I. Mian, J.H. Rowe, Review of hepatocellular carcinoma: epidemiology, etiology, and carcinogenesis, J. Carcinog. 16 (2017) 1.
[13] A. Giubellino, T.R. Burke Jr., D.P. Bottaro, Grb2 signaling in cell motility and cancer, Expert Opin. Ther. Targets 12 (2008) 1021–1033.
[14] R. Hao, P. Nanduri, Y. Rao, R.S. Panichelli, A. Ito, M. Yoshida, T.P. Yao, Proteasomes activate aggresome disassembly and clearance by producing unanchored ubiquitin chains, Mol. Cell 51 (2013) 819–828.
[15] S. Kaufhold, B. Bonavida, Central role of Snail1 in the regulation of EMT and resistance in cancer: a target for therapeutic intervention, J. Exp. Clin. Cancer Res. : CR (Clim. Res.) 33 (2014) 62.
[16] J. Li, T. Yakushi, F. Parlati, A.L. Mackinnon, C. Perez, Y. Ma, K.P. Carter, S. Colayco, G. Magnuson, B. Brown, K. Nguyen, S. Vasile, E. Suyama, L.H. Smith, E. Sergienko, A.B. Pinkerton, T.D.Y. Chung, A.E. Palmer, I. Pass, S. Hess, S.M. Cohen, R.J. Deshaies, Capzimin is a potent and specific inhibitor of proteasome isopeptidase Rpn11, Nat. Chem. Biol. 13 (2017) 486–493.
[17] G. Luo, N. Hu, X. Xia, J. Zhou, C. Ye, RPN11 deubiquitinase promotes proliferation and migration of breast cancer cells, Mol. Med. Rep. 16 (2017) 331–338.
[18] Z. Ma, X. Gao, W. Zhao, Y. Li, C. Li, C. Li, Relationship between expression of Pad1 homologue and multidrug resistance of idiopathic nephrotic syndrome, Pediatr. Int. : official journal of the Japan Pediatric Society 51 (2009) 732–735.
[19] K.D. Miller, R.L. Siegel, C.C. Lin, A.B. Mariotto, J.L. Kramer, J.H. Rowland, K.D. Stein, R. Alteri, A. Jemal, Cancer treatment and survivorship statistics, CA A Cancer J. Clin. 66 (2016) (2016) 271–289.
[20] P. Mitra, P. Kalailingam, H.B. Tan, T. Thanabalu, Overexpression of GRB2 enhances epithelial to mesenchymal transition of A549 cells by upregulating SNAIL expression, Cells (2018) 7.
[21] J.F. Nabhan, F.F. Hamdan, P. Ribeiro, A Schistosoma mansoni Pad1 homologue stabilizes c-Jun, Mol. Biochem. Parasitol. 121 (2002) 163–172.
[22] C. Perez, J. Li, F. Parlati, M. Rouffet, Y. Ma, A.L. Mackinnon, T.F. Chou, R.J. Deshaies, S.M. Cohen, Discovery of an inhibitor of the proteasome subunit Rpn11, J. Med. Chem. 60 (2017) 1343–1361.
[23] T. Schwarz, C. Sohn, B. Kaiser, E.D. Jensen, K.C. Mansky, The 19S proteasomal lid subunit POH1 enhances the transcriptional activation by Mitf in osteoclasts, J. Cell. Biochem. 109 (2010) 967–974.
[24] M.A. Smith, T. Licata, A. Lakhani, M.V. Garcia, H.U. Schildhaus, V. Vuaroqueaux, B. Halmos, A.C. Borczuk, Y.A. Chen, B.C. Creelan, T.A. Boyle, E.B. Haura, MET-GRB2 signaling-associated complexes correlate with oncogenic MET signaling and sensitivity to MET kinase inhibitors, Clin. Cancer Res. : an official journal of the American Association for Cancer Research 23 (2017) 7084–7096.
[25] Y. Song, S. Li, A. Ray, D.S. Das, J. Qi, M.K. Samur, Y.T. Tai, N. Munshi, R.D. Carrasco, D. Chauhan, K.C. Anderson, Blockade of deubiquitylating enzyme Rpn11 triggers apoptosis in multiple myeloma cells and overcomes bortezomib resistance, Oncogene 36 (2017) 5631–5638.
[26] J. Sun, S. Lu, M. Ouyang, L.J. Lin, Y. Zhuo, B. Liu, S. Chien, B.G. Neel, Y. Wang, Antagonism between binding site affinity and conformational dynamics tunes alternative cis-interactions within Shp2, Nat. Commun. 4 (2013) 2037.
[27] Z. Timsah, Z. Ahmed, C. Ivan, J. Berrout, M. Gagea, Y. Zhou, G.N. Pena, X. Hu, C. Vallien, C.V. Kingsley, Y. Lu, J.F. Hancock, J. Liu, A.B. Gladden, G.B. Mills, G. Lopez-Berestein, M.C. Hung, A.K. Sood, M. Bogdanov, J.E. Ladbury, Grb2 depletion under non-stimulated conditions inhibits PTEN, promotes Akt-induced tumor formation and contributes to poor prognosis in ovarian cancer, Oncogene 35 (2016) 2186–2196.
[28] Z.T. Tong, M.Y. Cai, X.G. Wang, L.L. Kong, S.J. Mai, Y.H. Liu, H.B. Zhang, Y.J. Liao, F. Zheng, W. Zhu, T.H. Liu, X.W. Bian, X.Y. Guan, M.C. Lin, M.S. Zeng, Y.X. Zeng, H.F. Kung, D. Xie, EZH2 supports nasopharyngeal carcinoma cell aggressiveness by forming a co-repressor complex with HDAC1/HDAC2 and Snail to inhibit E-cadherin, Oncogene 31 (2012) 583–594.
[29] A. Villanueva, V. Hernandez-Gea, J.M. Llovet, Medical therapies for hepatocellular carcinoma: a critical view of the evidence, Nat. Rev. Gastroenterol. Hepatol. 10 (2013) 34–42.
[30] B. Wang, A. Ma, L. Zhang, W.L. Jin, Y. Qian, G. Xu, B. Qiu, Z. Yang, Y. Liu, Q. Xia, Y. Liu, POH1 deubiquitylates and stabilizes E2F1 to promote tumour formation, Nat. Commun. 6 (2015) 8704.
[31] B. Wang, X. Xu, Z. Yang, L. Zhang, Y. Liu, A. Ma, G. Xu, M. Tang, T. Jing, L. Wu, Y. Liu, POH1 Contributes to Hyperactivation of TGF-Beta Signaling and Facilitates Hepatocellular Carcinoma Metastasis through Deubiquitinating TGF-Beta Receptors and Caveolin-1, EBioMedicine, 2019.
[32] B. Wang, X. Xu, Z. Yang, L. Zhang, Y. Liu, A. Ma, G. Xu, M. Tang, T. Jing, L. Wu, Y. Liu, POH1 contributes to hyperactivation of TGF-beta signaling and facilitates hepatocellular carcinoma metastasis through deubiquitinating TGF-beta receptors and caveolin-1, EBioMedicine 41 (2019) 320–332.
[33] C.H. Wang, S.X. Lu, L.L. Liu, Y. Li, X. Yang, Y.F. He, S.L. Chen, S.H. Cai, H. Wang, J.P. Yun, POH1 knockdown induces cancer cell apoptosis via p53 and bim, Neoplasia 20 (2018) 411–424.
[34] R. Zhu, Y. Liu, H. Zhou, L. Li, Y. Li, F. Ding, X. Cao, Z. Liu, Deubiquitinating enzyme PSMD14 promotes tumor metastasis through stabilizing SNAIL in human esophageal squamous cell carcinoma, Cancer Lett. 418 (2018) 125–134.